

LEVEL

12

OSU

EIGENFUNCTIONS OF HERMITIAN ITERATED OPERATORS WITH
APPLICATION TO DISCRETE AND CONTINUOUS
RADIATING SYSTEMS

The Ohio State University

Naoki Inagaki and Robert J. Garbacz

The Ohio State University

ElectroScience Laboratory

Department of Electrical Engineering
Columbus, Ohio 43212

AD A100591

DTIC FILE COPY

TECHNICAL REPORT 712695-1

Contract N00014-78-C-0049

January 1981

DTIC
ELECTE
JUN 25 1981
S D

Dept. of the Navy
Office of Naval Research
Arlington, Virginia 22217

DTIC REPORT 712695-1

Approved for public release

Distribution unlimited

81 6 01 089

NOTICES

When Government drawings, specifications, or other data are used for any purpose other than in connection with a definitely related Government procurement operation, the United States Government thereby incurs no responsibility nor any obligation whatsoever, and the fact that the Government may have formulated, furnished, or in any way supplied the said drawings, specifications, or other data, is not to be regarded by implication or otherwise as in any manner licensing the holder or any other person or corporation, or conveying any rights or permission to manufacture, use, or sell any patented invention that may in any way be related thereto.

UNCLASSIFIED

SECURITY CLASSIFICATION OF THIS PAGE (When Data Entered)

REPORT DOCUMENTATION PAGE		READ INSTRUCTIONS BEFORE COMPLETING FORM
1. REPORT NUMBER	2. GOVT ACCESSION NO.	3. RECIPIENT'S CATALOG NUMBER
	AD-A700592	
4. TITLE (and Subtitle)	5. TYPE OF REPORT & PERIOD COVERED	
6. EIGENFUNCTIONS OF HERMITIAN ITERATED OPERATORS WITH APPLICATION TO DISCRETE AND CONTINUOUS RADIATING SYSTEMS.	9 Technical Report	
7. AUTHOR(s)	6. PERFORMING ORG. REPORT NUMBER	
10 Naoki Inagaki Robert J. Garbacz	14 ESL-712695-1	
	8. CONTRACT OR GRANT NUMBER(s)	
	13 Contract N00014-78-C-0049	
9. PERFORMING ORGANIZATION NAME AND ADDRESS	10. PROGRAM ELEMENT PROJECT, TASK AREA & WORK UNIT NUMBERS	
The Ohio State University ElectroScience Laboratory, Department of Electrical Engineering Columbus, Ohio 43212	12 12421	
11. CONTROLLING OFFICE NAME AND ADDRESS	12. REPORT DATE	
Dept. of the Navy, Office of Naval Research, 800 Quincy Street Arlington, VA 22217	11 January 1981	
	13. NUMBER OF PAGES	
	36	
14. MONITORING AGENCY NAME & ADDRESS (if different from Controlling Office)	15. SECURITY CLASS. (of this report)	
	Unclassified	
	15a. DECLASSIFICATION/DOWNGRADING SCHEDULE	
16. DISTRIBUTION STATEMENT (of this Report)		
17. DISTRIBUTION STATEMENT (of the abstract entered in Block 20, if different from Report)		
18. SUPPLEMENTARY NOTES		
19. KEY WORDS (Continue on reverse side if necessary and identify by block number)		
Eigenfunctions Aperture antennas Hermitian operator Antennas Characteristic modes Arrays Modes Impedance Scatterers Iterated operator		
20. ABSTRACT (Continue on reverse side if necessary and identify by block number)		
In this report we study some properties and applications of Hermitian operators formed by the iteration of any given operator with its adjoint. Such a given operator might arise in array and aperture antenna theory and, as shown in examples, the eigenfunctions of the corresponding Hermitian iterated operator can be used to maximize power transferred from an array to a point, or from one aperture to a second aperture. Constraints, such as a normed power source radiating into a speci-		

DD FORM 1 JAN 73 1473 EDITION OF 1 NOV 65 IS OBSOLETE

UNCLASSIFIED

SECURITY CLASSIFICATION OF THIS PAGE (When Data Entered)

UNCLASSIFIED

SECURITY CLASSIFICATION OF THIS PAGE(When Data Entered)

20..

fied sector of space, may be incorporated into the theory as well, as illustrated by an example. The eigencurrents and fields of Hermitian iterated operators associated with perfectly conducting bodies are introduced and contrasted with the characteristic currents and fields of Garbacz, Harrington, and Mautz.

Accession For	
NTIS GRA&I	<input checked="" type="checkbox"/>
DTIC TAB	<input type="checkbox"/>
Unannounced	<input type="checkbox"/>
Justification	
By <u>Per Ltr. on file</u>	
Distribution/	
Availability Codes	
Dist	Avail and/or Special
A	

DTIC
ELECTE
JUN 25 1981
D

UNCLASSIFIED

SECURITY CLASSIFICATION OF THIS PAGE(When Data Entered)

TABLE OF CONTENTS

	Page
I INTRODUCTION	1
II EIGENFUNCTIONS ASSOCIATED WITH SOURCE AND FIELD	2
A. <u>Eigenvalue Equation of a</u>	6
<u>Hermitian Iterated Operator</u>	3
B. <u>Eigensources and Eigenpatterns of Arrays</u>	6
C. <u>Focussing the Field of an Array</u>	8
D. <u>Eigensources and Eigenfields of a</u>	12
<u>Slit Aperture</u>	
III EIGENVALUE EQUATION WITH HERMITIAN WEIGHT OPERATOR	18
A. <u>Maximizing Endfire Radiation of an Array</u>	21
<u>While Fixing the Radiated Power in a</u>	
<u>Specified Angular Sector</u>	
IV EIGENVALUE EQUATION OF PERFECTLY	23
CONDUCTING BODIES	
V CONCLUSIONS	34
REFERENCES	35

I. INTRODUCTION

Problems of analysis and synthesis of radiating systems require appropriate functions in which to expand a source distribution and associated radiated field. To be most useful it is desirable that such functions be suitable for source and field representations simultaneously, that they be complete and that they be orthogonal in some sense over both the source and field region of interest. In the familiar case when the regions of the source and the field coincide with coordinate surfaces of coordinate systems in which the Helmholtz equation is separable, the corresponding eigenfunction representation is valid for both the source and the field. The characteristic modes of loss-free bodies of arbitrary shape, introduced by Garbacz [1,2], and elaborated by Harrington and Mautz [3,4] give another possible representation where the source and field observation regions coincide, but the orthogonal properties of these functions apply only to the body surface and the sphere at infinity.

In this report we treat the more general case where the region of observation does not necessarily coincide with the source region, resulting in orthogonal properties over more general regions than the body surface and the sphere at infinity. An investigation of the validity of Parseval's relation for a more general operator equation than a Fourier transform leads us to an eigenvalue equation of the Hermitian iterated operator, whose solutions shall be called eigensources and the radiated fields of which shall be called eigenfields. An eigensource and an associated eigenfield each satisfies an orthogonality property simultaneously but, in general, over different regions of space. The sets of eigensources and eigenfields can then be used as convenient basic functions with which to solve various problems systematically.

Examples are developed for the optimization of an array under given constraints and for the determination of aperture distributions

transferring maximum power to a second aperture. In the latter case, the eigenfunctions arising from the present theory are shown to be the prolate spheroidal functions. In the case where the eigenequation is developed from a current source flowing on a closed surface and the component of the corresponding electric field tangential to the same surface, we are led to eigencurrents and eigenfields which differ from characteristic modes (which involve the same two quantities); whereas a characteristic current and a characteristic field display differing amplitude distributions but maintain a constant phase relationship over the surface, the eigencurrents and eigenfields introduced here display similar amplitude distributions but maintain a complex conjugate phase relationship over the surface [5]. Only when the surface corresponds to a coordinate of the coordinate systems where separability applies do the characteristic functions and the eigenfunctions of the Hermitian iterated operator coalesce to become one and the same such as in the case of the circular conducting cylinder and conducting sphere. Examples are discussed involving the infinite rectangular conducting cylinder, and the linear conductor.

II. EIGENFUNCTIONS ASSOCIATED WITH SOURCE AND FIELD

We consider a source s and a resulting field f all in a linear medium which are related by an integral operator G as

$$f = Gs \quad (1)$$

When the operator equation (1) happens to be a Fourier transform (when for example s is a planar source and f is the corresponding far field on the sphere at infinity) we know that f and s satisfy a Parseval's relation, i.e., the norm of f is equal to the norm of s . In the following section we inquire whether or not this same result applies to the more general operator equation (1).

A. Eigenvalue Equation of a Hermitian Iterated Operator

To begin, let us define the inner product of two sources, (s_i, s_j) and the inner product of two fields (f_i, f_j) as follows:

$$(s_i, s_j)_{R_s} = \int_{R_s} s_i(kx) s_j^c(kx) d(kx) \quad (2)$$

$$(f_i, f_j)_{R_f} = \int_{R_f} w(kx) f_i(kx) f_j^c(kx) d(kx) \quad (3)$$

where $w(kx)$ is a real weight function (often unity) and R_s and R_f are the regions where the sources are distributed and the fields are observed, respectively. The superscript c denotes complex conjugate and $k = \frac{2\pi}{\lambda}$ is the wavenumber in terms of the wavelength λ .

Using Equation (1), we obtain

$$\begin{aligned} (f_i, f_j)_{R_f} &= (Gs_i, Gs_j)_{R_f} \\ &= (s_i, G^*Gs_j)_{R_s}, \end{aligned} \quad (4)$$

where G^* is the adjoint operator of G . The iterated operator G^*G is Hermitian and is denoted henceforth by[†]

$$H \equiv G^*G. \quad (5)$$

[†]More explicitly, since G is an integral operator, Equation (1) is of the form

$$f(kx) = Gs(kx') = \int_{R_s} G(kx, kx') s(kx') d(kx')$$

(Footnote Continued)

where G is the integral kernel. Therefore Equation (3) becomes

$$\begin{aligned} (f_i, f_j)_{R_f} &= \int_{R_f} w(kx) \left[\int_{R_s} G(kx, kx') s_i(kx') d(kx') \right] \left[\int_{R_s} G^C(kx, kx'') s_j^C(kx'') d(kx'') \right] d(kx) \\ &= \int_{R_s} s_i(kx') \left\{ \int_{R_s} \int_{R_f} w(kx) G(kx, kx') G^C(kx, kx'') d(kx) \right\} s_j^C(kx'') d(kx'') d(kx') \\ (s_i, G^* G s_j)_{R_s} &= \int_{R_s} s_i(kx') \left\{ \int_{R_s} \int_{R_f} w^C(kx) G^C(kx, kx') G(kx, kx'') d(kx) \right\} s_j(kx'') d(kx'') d(kx') \end{aligned}$$

where we have used Equation (4) on the left side of the above equation. Understanding that the inner product over the source region R_s is defined by Equation (2) and comparing the two sides of this equation, we see that

$$H s_j(kx') = G^* G s_j(kx') = \int_{R_s} \int_{R_f} w(kx) G^C(kx, kx') G(kx, kx'') d(kx) s_j(kx'') d(kx'').$$

In this expression we recognize that $w^C(kx) = w(kx)$ because the weighting function $w(kx)$ is real. It is more usual to define an iterated operator without the weighting function.

If G is the Fourier operator, H reduces to an identity operator and Equation (4) is Parseval's relation. For a similar relation to hold in our case with a more general operator, the source must satisfy an equation of the form

$$Hs_i = v_i s_i \quad (6)$$

whence Equation (4) becomes

$$(f_i, f_j)_{R_f} = v_i (s_i, s_j)_{R_s} \quad (7)$$

We recognize Equation (6) as an eigenvalue equation of H with eigenvalues v_i and eigenfunction solutions s_i which satisfy the orthonormality condition

$$(s_i, s_j)_{R_s} = \delta_{ij} \quad (8)$$

where δ_{ij} is the Kronecker delta. From Equations (4), (7) and (8) we also have

$$(f_i, f_j)_{R_f} = (s_i, Hs_j)_{R_s} = v_i \delta_{ij} \quad (9)$$

We shall call $\{s_i\}$ the eigensources defined on R_s and $\{f_i\}$ the eigenfields defined on R_f . The iterated Hermitian operator property of H assures us that the $\{v_i\}$ are real and positive semidefinite and that the $\{s_i\}$ are orthogonal and complete on R_s if H is not improperly singular. The same may be said of the $\{f_i\}$. We shall order the eigenvalues $\{v_i\}$ such that their values decrease with increasing index i . This, together with Equations (8) and (9), implies that the ratio of the norm of f_i to the norm of s_i is largest for the lowest eigenvalue v_i and equal to it numerically.

Now that we have defined pertinent quantities in general terms, let us consider a few simple but useful examples of the above theory. In the following sections an $e^{+j\omega t}$ time convention is assumed and suppressed.

B. Eigenources and Eigenpatterns of Arrays

Figure 1 shows an N-element linear array of isotropic point sources with uniform spacing d . We consider the source s to be the N array elements with excitation strengths $s_1, s_2 \dots s_N$ defined on the array proper, and the field f to be the corresponding far-radiated field pattern function $f(\theta)$ defined on the sphere at infinity. In this case the operator Equation (1) becomes

$$f(\theta) = \sum_{n=1}^N G_\theta(n) s_n, \quad (10)$$

with

$$G_\theta(n) = e^{jnkdcos\theta}, \quad n=1,2,\dots,N \quad (11)$$

and Equations (2) and (3) become

$$(s,s)_{R_s} = \sum_{n=1}^N s_n s_n^C \quad (12)$$

$$(f,f)_{R_f} = 2\pi \int_0^\pi f(\theta) f^C(\theta) \sin\theta d\theta \quad (13)$$

The weight function w in this case is $2\pi \sin\theta$. The eigenvalue equation (6) reduces to the algebraic equation

$$\sum_{m=1}^N H(n,m) s_{im} = \lambda_i s_{in}, \quad i,n=1,2,\dots,N \quad (14)$$

where the operator H reduces to an $N \times N$ matrix H with elements

$$\begin{aligned} H(n,m) &= 2\pi \int_0^\pi G_\theta(n) G_\theta^C(m) \sin\theta d\theta \\ &= 4\pi \frac{\sin(n-m)kd}{(n-m)kd} \quad n,m=1,2,\dots,N \end{aligned} \quad (15)$$

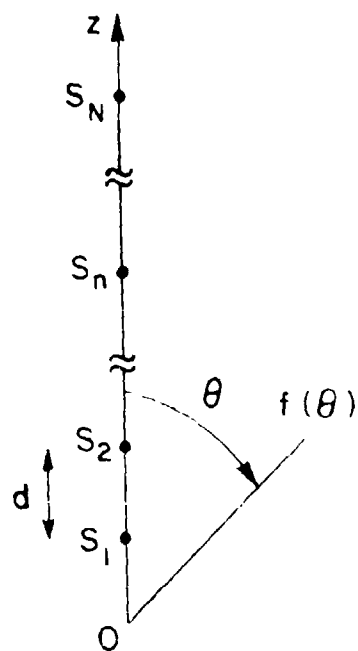


Figure 1. N-element linear array antenna with spacing d .

The eigenpattern $f_i(\theta)$ corresponding to the i th eigensource s_i is

$$f_i(\theta) = \sum_{n=1}^N G_\theta(n) s_{in} \quad (16)$$

The sets $\{s_i\}$ and $\{f_i\}$ are useful in at least two ways. First, the eigensource with the largest eigenvalue is the source which radiates the largest power while the norm of the source is fixed, i.e., the array has the highest radiation efficiency. Secondly, we can synthesize a given arbitrary pattern $f(\theta)$ in a least mean square sense by choosing the N source excitations in Equation (11) to be

$$s_n = \sum_{i=1}^N \frac{(f, f_i)}{\lambda_i} s_{in} \quad n=1, 2, \dots, N. \quad (17)$$

Figures 2 and 3 show calculated eigensources and eigenpattern magnitudes for $N=5$, $d=0.4\lambda$.

C. Focussing the Field of an Array

As a second example consider the same linear array discussed above, but whose field is observed at a point P in the near field region as pictured in Figure 4. Here, the appropriate μ operator reduces to a $1 \times N$ matrix with elements

$$G_1(n) = \frac{e^{-jkr_n}}{kr_n} \quad n=1, 2, \dots, N \quad (18)$$

where the r_n are defined in Figure 4, and the operator μ reduces to an $N \times N$ matrix with elements

$$H(n, m) = \frac{e^{jk(r_n - r_m)}}{k^2 r_n r_m} \quad n, m=1, 2, \dots, N \quad (19)$$

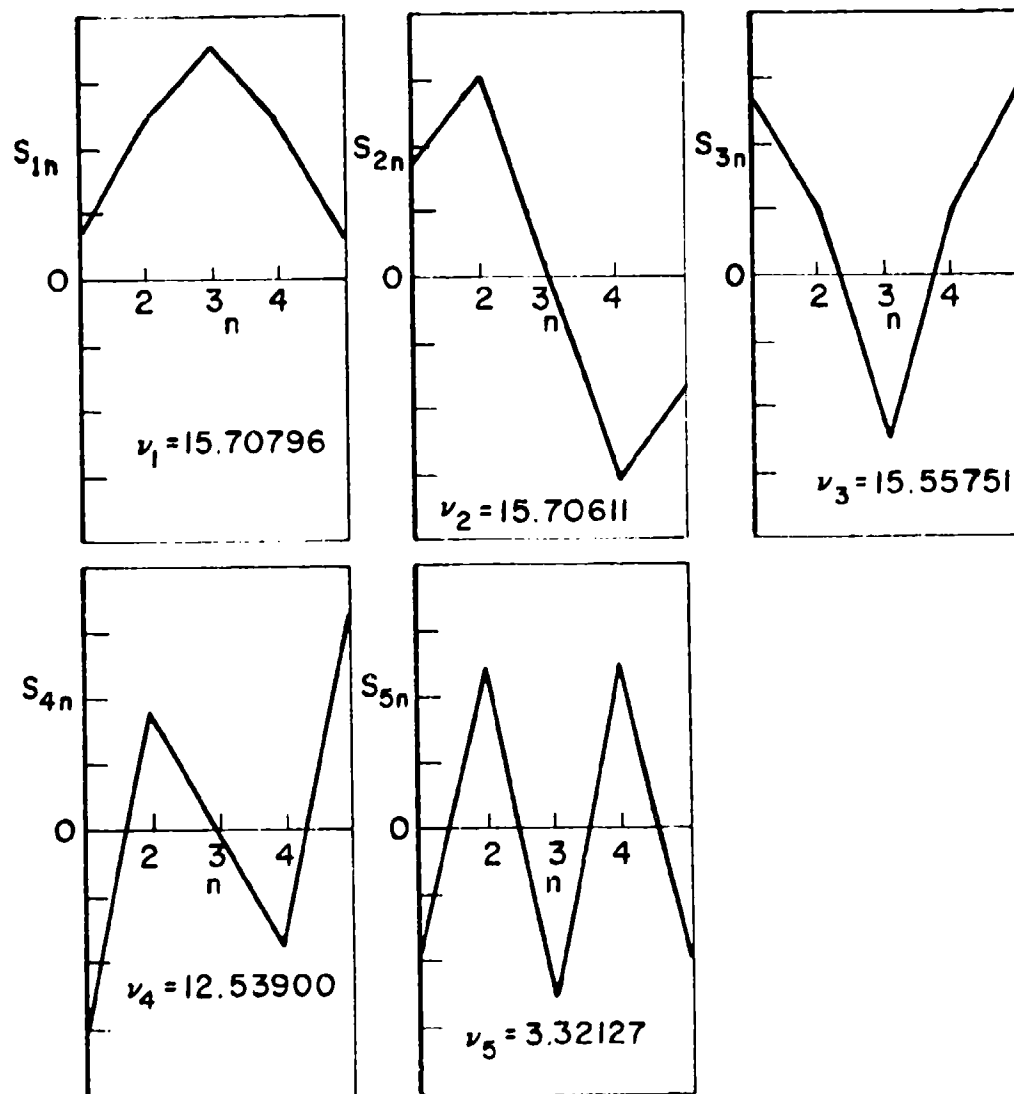


Figure 2. Eigensources of five element linear array with $d=0.4\lambda$.

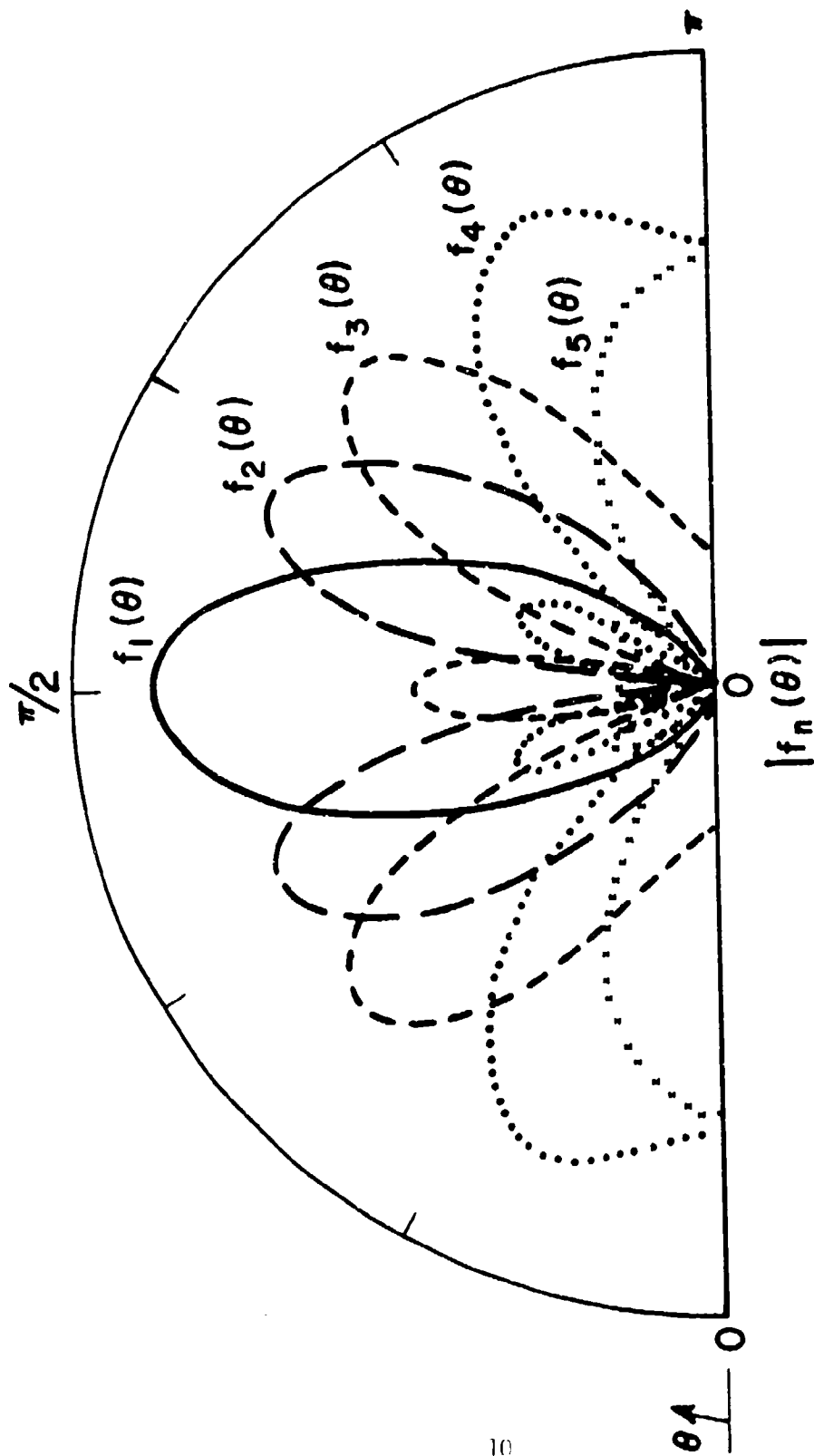


Figure 3. Eigenpatterns corresponding to the eigensources of Figure 2.

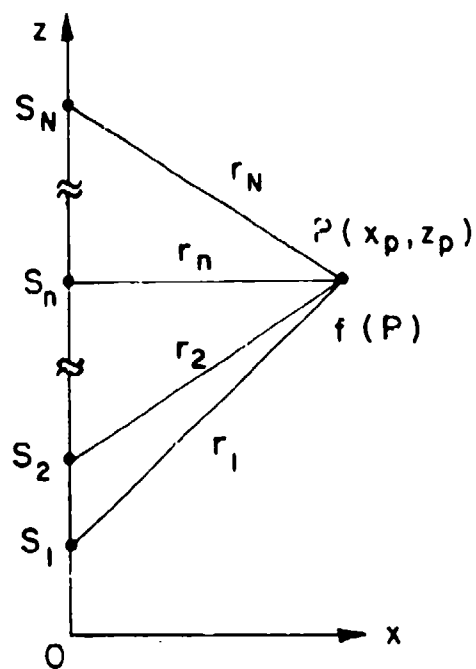


Figure 4. N-element linear array antenna and an observation point P located in the near field region.

The norm of s remains the same as Equation (12) but because region R_f in this case is the near field point P the norm on f becomes simply

$$(f, f)_P = f(P)f^C(P) \quad (20)$$

It is obvious that the eigensource with the largest eigenvalue yields the largest field at point P while the norm of the source is fixed. Figure 5 shows this case of an optimally focussed linear array with $N=5$, $d=0.5\lambda$ and P located at $(2\lambda, 1.5\lambda) = (x_P, z_P)$. We comment that the optimum field at P is larger by 0.11 dB than is the field obtained there from an array of co-phased elements with uniform amplitudes.

D. Eigensources and Eigenfields of a Slit Aperture

As an example of a continuously distributed radiating system, consider two identical planar parallel slits of width $2a$ and separation b , as shown in Figure 6. The left slit is considered to form a source and the right slit serves to observe the field due to the source. For such a two dimensional problem \mathcal{G} is the integral operator [6]

$$f(kx_2) = \int_{-ka}^{ka} G(kx_2, kx_1) s(kx_1) d(kx_1) \quad (21)$$

with kernel

$$G(kx_2, kx_1) = \frac{e^{j\frac{\pi}{4}}}{2\pi} \sqrt{\frac{\lambda}{b}} e^{-jk \frac{(x_1 - x_2)^2}{2b}} \quad (22)$$

The Fresnel approximation has been assumed in Equation (22). The Hermitian iterated operator \mathcal{H} is an integral operator with kernel

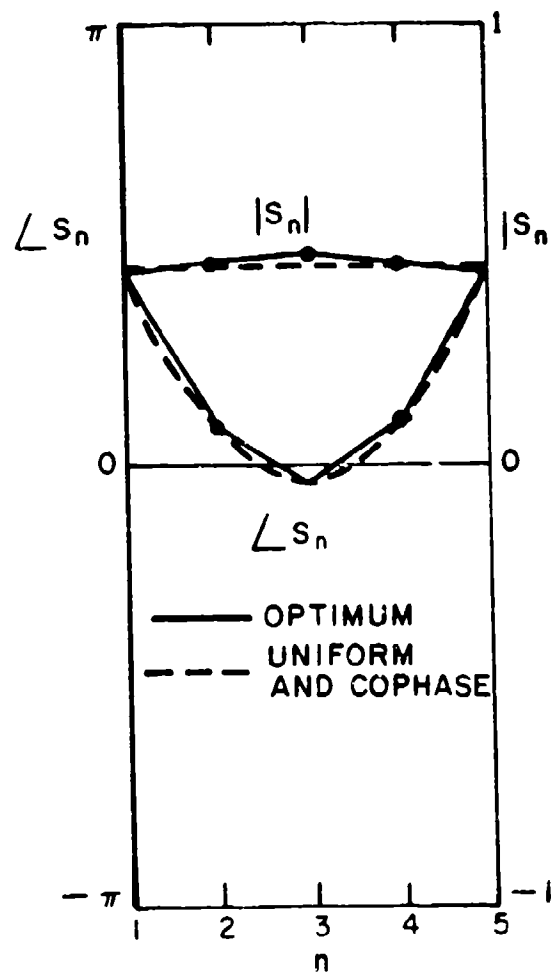


Figure 5. Optimum source distribution of five element linear array antenna focussed in the near field region compared with uniform amplitude and cophase distribution.

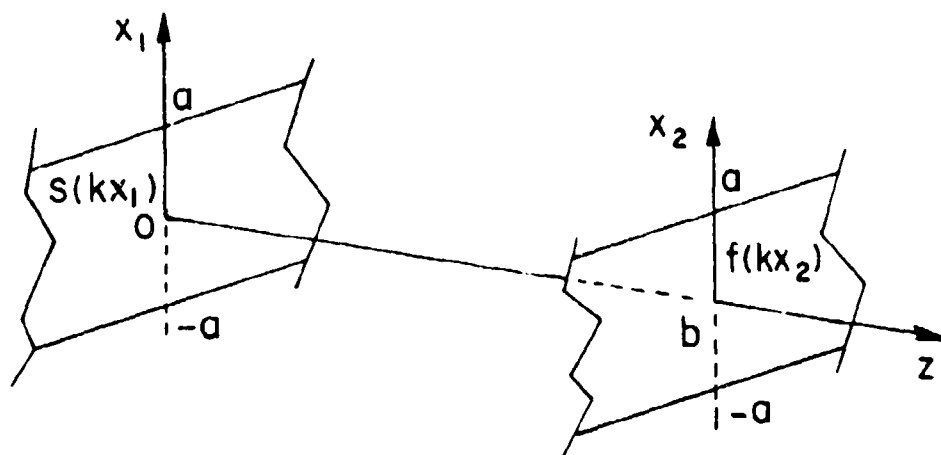


Figure 6. Two apertures with width $2a$ and separation b .

$$\begin{aligned}
H(kx'_1, kx''_1) &= \int_{-ka}^{ka} G^C(kx_2, kx'_1) G(kx_2, kx''_1) d(kx_2) \\
&= \frac{a}{\pi b} \left[e^{+jk \frac{x'^2_1 - x''^2_1}{2b}} \right] \left[\frac{\sin \frac{ka}{b}(x'_1 - x''_1)}{\frac{ka}{b}(x'_1 - x''_1)} \right]. \quad (23)
\end{aligned}$$

Defining a modified source function $r(kx_1)$ and a real symmetric kernel $h(kx'_1, kx''_1)$ by

$$r(kx_1) \equiv e^{-j \frac{(kx_1)^2}{2kb}} s(kx_1) \quad (24)$$

$$h(kx'_1, kx''_1) \equiv \frac{a}{\pi b} \left[\frac{\sin \frac{a}{b}(kx'_1 - kx''_1)}{\frac{a}{b}(kx'_1 - kx''_1)} \right], \quad (25)$$

the eigenvalue equation (6) becomes

$$\int_{-ka}^{ka} h(kx'_1, kx''_1) r_i(kx''_1) d(kx''_1) = v_i r_i(kx'_1), \quad i = 0, 1, 2, \dots \quad (26)$$

Once this equation is solved for $\{r_i\}$, the set of eigensources $\{s_i\}$ and eigenfields $\{f_i\}$ are given, respectively, by

$$s_i(kx_1) = N_i r_i(kx_1) e^{+j \frac{(kx_1)^2}{2kb}} \quad (27)$$

and

$$\begin{aligned}
 f_i(kx_2) &= N_i \int_{-ka}^{ka} G(kx_2, kx_1) s_i(kx_1) d(kx_1) \\
 &= N_i \frac{e^{-j \left[\frac{(kx_2)^2}{2kb} - \frac{\pi}{4} \right]}}{2\pi} \sqrt{\frac{\lambda}{b}} \int_{-ka}^{ka} e^{+j \frac{kx_2 kx_1}{kb}} r_i(kx_1) d(kx_1)
 \end{aligned} \tag{28}$$

where N_i are convenient normalizing constants. With a change of variables

$$ka = \frac{T}{2} \tag{29}$$

$$\frac{a}{b} = \Omega \tag{30}$$

$$kx_1' = t \tag{31}$$

$$kx_1'' = s, \tag{32}$$

equation (26) may be rewritten in the form

$$\int_{-T/2}^{T/2} \frac{\sin \Omega(t-s)}{\pi(t-s)} r_i(s) ds = v_i r_i(t), \quad i = 0, 1, 2, \dots \tag{33}$$

This equation has been studied extensively by Slepian and Pollak [7] who show its solutions to be the angular prolate spheroidal functions, $r_i(t) = S_{0i}(c, t)$ and its eigenvalues to be

$$v_i(c) = \frac{2c}{\pi} \left[R_{0i}^{(1)}(c, 1) \right]^2, \quad i = 0, 1, 2, \dots \tag{34}$$

where $R_{0i}^{(1)}(c,1)$ are radial prolate spheroidal functions. The parameter $c = \frac{\Omega T}{2}$ or, according to Equations (29) and (30), $c = \frac{2\pi a^2}{\lambda b} = 2\pi F$ where F is the Fresnel number

$$F = \frac{a^2}{\lambda b} \quad (35)$$

Asymptotic expressions for $\lambda_i(c)$ for small and large values of c (i.e., small and large values of the Fresnel number) with index i being fixed have been derived by Slepian and Sonnenblack [8].

For the normalization condition expressed by Equation (8) to hold, the i th eigensource is

$$s_i(kx_1) = v_i^{-1/2}(c) e^{j \frac{(kx_1)^2}{2kb}} S_{0i}(c, kx_1) \quad (36)$$

and the corresponding eigenfield given by Equation (28) is

$$\begin{aligned} f_i(kx_2) &= v_i^{-1/2}(c) e^{-j \left[\frac{(kx_2)^2}{2kb} - \frac{\pi}{4} - \frac{n\pi}{2} \right]} \sqrt{\frac{2c}{\pi}} R_{on}^{(1)}(c,1) S_{0i}(c, kx_2) \\ &= \left\{ e^{-j \left[\frac{(kx_2)^2}{2kb} - \frac{\pi}{4} - \frac{n\pi}{2} \right]} S_{0i}(c, kx_2) \right\} \operatorname{sgn} \left[R_{on}^{(1)}(c,1) \right]. \quad (37) \end{aligned}$$

Since the $\{S_{0i}\}$ form a complete orthogonal set on either slit, a source and its field are conveniently expanded in terms of $\{s_i\}$ and $\{f_i\}$, respectively. The eigenvalue $v_i(c)$ corresponds to the ratio of the power received to the power transmitted in the i th mode. Furthermore, the $i=0$ mode has the largest eigenvalue, $v_0(c)$, from which we conclude that power transfer between apertures is maximized in this lowest order mode. Using this fact and the fact [8] that for small c (i.e., small F),

$$v_0(c) \approx \frac{2c}{\pi} = 4F, \quad (38)$$

we can state that for two distantly separated slits the received power cannot exceed $4F$ times the transmitted power. For large c (i.e., large F) it is known [8] that

$$v_0(c) \approx 1 - 4\sqrt{\pi c} e^{-2c} = 1 - 4\pi\sqrt{2F} e^{-4\pi F} \quad (39)$$

which has a value only slightly less than 1 for F values larger than $F = 1/2$.

It is worthwhile to note that the lowest order (optimum) source has a positive-going parabolic phase distribution (Equation (27)) which tends to compensate for the diverging effect of a finite slit; the field achieved by this optimum source has a negative-going phase distribution (Equation (28)).

III. EIGENVALUE EQUATION WITH HERMITIAN WEIGHT OPERATOR

It has been shown in the previous sections that the eigenvalue equation of the Hermitian iterated operator yields eigensources and eigenfields which can form useful basic sets in which to expand arbitrary source and field distributions. It was also shown that an optimum source can be determined which produces maximum-field over the designated field region under the condition that the norm of the source is fixed. In this section we extend the theory to encompass more general conditions by replacing Equation (6) by an eigenvalue equation of the Hermitian iterated operator which includes a Hermitian weight operator, i.e.,

$$HS_i = v_i \hat{H} S_i \quad (40)$$

Here we assume that the weight operator \hat{H} is Hermitian and positive definite in which case it can be shown that the solutions of Equation (40) satisfy the relations

$$(s_i, \hat{H} s_j)_{R_S} = \delta_{ij} \quad (41)$$

$$(s_i, H s_j)_{R_S} = v_i \delta_{ij} \quad (42)$$

Equations (40), (41), and (42) are extensions of Equations (6), (8), and (9), respectively. Thus, we can interpret the eigensource with the largest eigenvalue as being the optimum source in the sense that $(s, H s)_{R_S}$ is largest, $(s, \hat{H} s)_{R_S}$ being fixed (rather than $(s, s)_{R_S}$ being fixed as developed in Section II).

In work to follow on arrays it will be useful to articulate the operators in Equation (40) in the form of matrices. If U is the orthogonal matrix which diagonalizes \hat{H} and μ is the diagonalized matrix, i.e.,

$$U^* \hat{H} U = \mu = \begin{bmatrix} \mu_1 & & & \\ & \ddots & & \\ & & \mu_n & \\ & & & \ddots \\ & & & & \mu_N \end{bmatrix}, \quad (43)$$

then Equation (40) transforms to

$$(\mu^{-1/2} U^* H U \mu^{-1/2}) (\mu^{1/2} U^* s_i) = v_i (\mu^{1/2} U^* s_i), \quad (44)$$

or

$$H' s'_i = v_i s'_i \quad (45)$$

whose eigenvalues satisfy the orthogonality condition

$$(s'_i, s'_j)_{R_S} = \delta_{ij} \quad (46)$$

It is easy to verify that Equations (45) and (46) are consistent with Equations (42) and (41), respectively.

A second useful case arises when \hat{H} , in addition to being Hermitian and positive definite, is also factorizable as

$$\hat{H} = A^* A \quad . \quad (47)$$

Equation (40) then transforms to

$$(A^{-1*} \hat{H} A^{-1})(A s_i) = v_i (A s_i) \quad (48)$$

or

$$H'' s_i'' = v_i s_i'' \quad (49)$$

whose eigensolutions satisfy the orthonormality condition

$$(s_i'', s_j'')_{R_S} = \delta_{ij} \quad . \quad (50)$$

It is easy to verify that Equations (49) and (50) lead back to Equations (42) and (41), respectively. In addition it can be shown [9] that when \hat{H} is factorizable the minimum eigenvalue is (in matrix notation)

$$v_{\min} = (A H^{-1} A^*)^{-1} \quad (51)$$

and the corresponding eigensource is

$$s_{\min} = H^{-1} A^* \quad . \quad (52)$$

A. Maximizing Endfire Radiation of an Array
While Fixing the Radiated Power in a
Specified Angular Sector

A linear array of N isotropic point sources equispaced a distance d along the z -axis as sketched in Figure 1 radiates into the conical sector about endfire shown in Figure 7. The power radiated is given by

$$\begin{aligned}\hat{P} &= 2\pi \sum_{m=1}^N \sum_{n=1}^N s_m s_n^c \int_{\theta_0}^{\pi} e^{j(m-n)kd\cos\theta} \sin\theta \, d\theta \\ &= \sum_{m=1}^N \sum_{n=1}^N s_m \left[\hat{H}(m,n) s_n \right]^c\end{aligned}\quad (53)$$

where

$$\hat{H}(m,n) = 2\pi e^{-j(m-n)\frac{kd}{2}(\cos\theta_0-1)} \frac{\sin\left[(m-n)\frac{kd}{2}(1+\cos\theta_0)\right]}{(m-n)\frac{kd}{2}}\quad (54)$$

$\hat{H}(m,n)$ are the elements of an $N \times N$ Hermitian matrix A . It is clear that \hat{P} appears in the form

$$\hat{P} = (s, \hat{H}s)_{R_s}\quad (55)$$

which, if we constrain \hat{P} to be unity, corresponds to Equation (41). Similarly, the power density radiated in the endfire direction, $\theta=\pi$, is

$$S = (s, Hs)_{R_s}\quad (56)$$

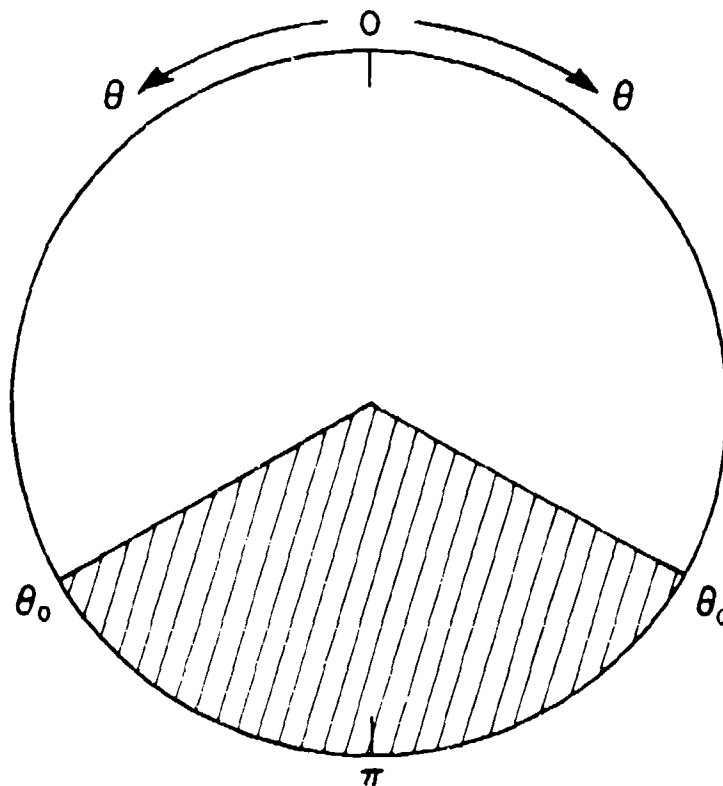


Figure 7. Angular sector (shaded) in which radiated power is to be confined.

where H is an $N \times N$ matrix whose elements are

$$H(m,n) = e^{-j(m-n)kd} \quad (57)$$

The optimum source, that is, the source which maximizes the end-fire power density S while constraining the radiated power \hat{P} to a specified sector is the eigensource with the largest eigenvalue satisfying Equation (40) with \hat{H} and H specified by matrix elements given in Equations (54) and (57), respectively. Field patterns for an example with $N=5$, $d=0.3\lambda$, $\theta_0=30^\circ(30^\circ)120^\circ$ are shown in Figures 8-10.

IV. EIGENVALUE EQUATION OF PERFECTLY CONDUCTING BODIES

Garbacz investigated a generalized expansion for the field radiated or scattered by a loss-free obstacle of arbitrary shape S in terms of characteristic functions defined in Ref. [1]. He noted for the perfectly conducting obstacle that each characteristic function is associated with a real characteristic current defined on S which gives rise to equiphase fields throughout the volume occupied by the obstacle. This observation, though not proven in a general way, led him to obtain a characteristic equation

$$X J_i = \lambda_i R J_i \quad (58a)$$

or

$$E_i = Z J_i = (1+j\lambda_i) R J_i \quad (58b)$$

where J_i is the i th characteristic current associated with the i th characteristic value λ_i and R and X are the Real and Imaginary Hermitian parts

$$R = \frac{1}{2}(Z+Z^G) \quad (59)$$

$$X = -j \frac{1}{2}(Z-Z^G) \quad (60)$$

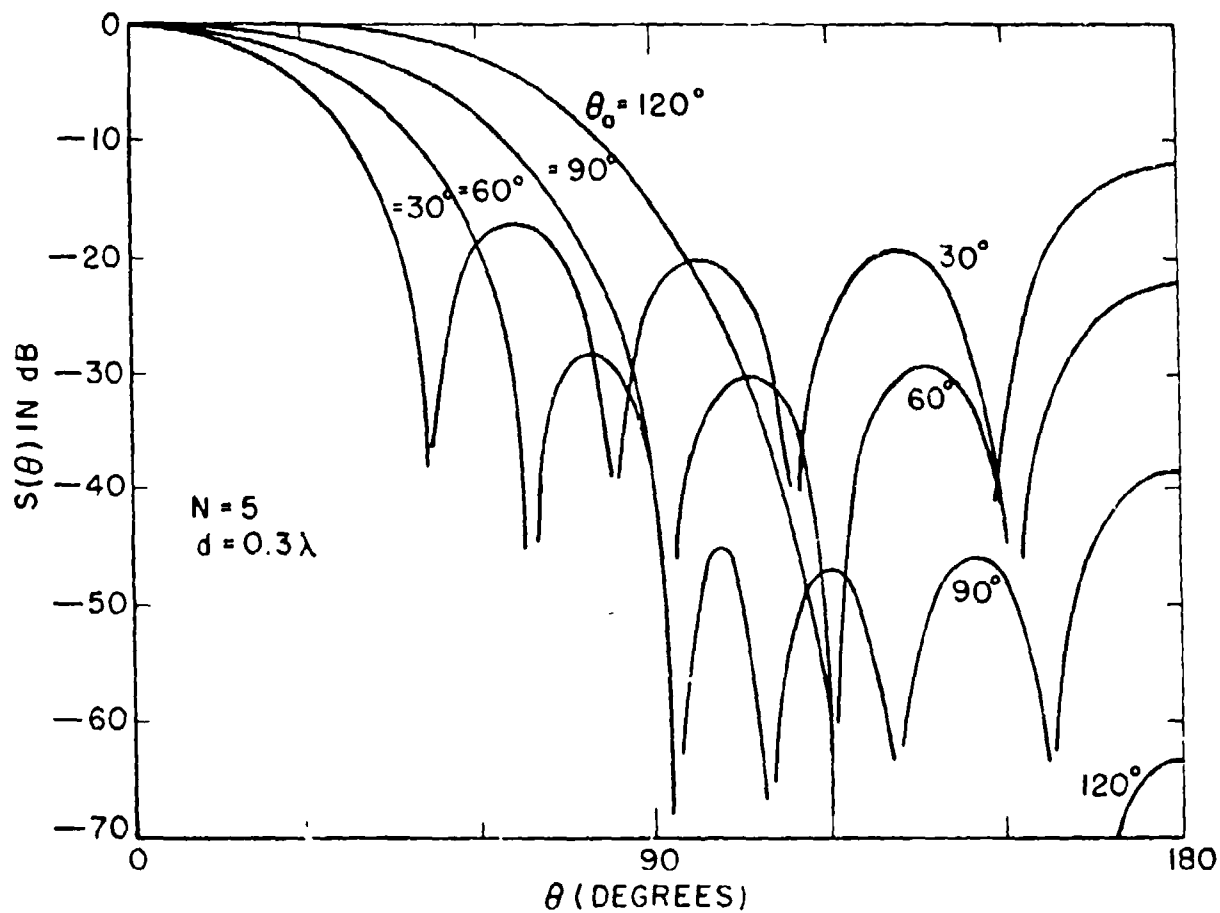


Figure 8. Optimum field radiation patterns of an array whose radiated power in a sector of angle (θ_0, π) is minimized while the endfire radiation intensity is fixed.

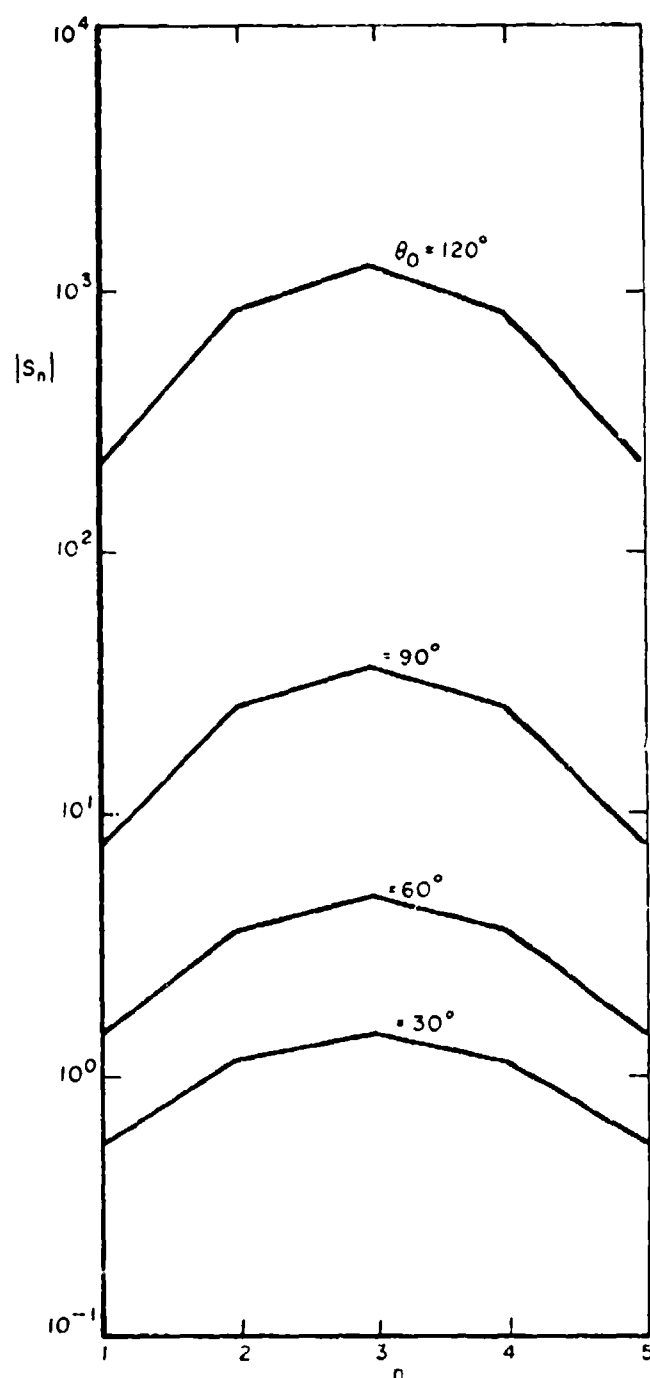


Figure 9. The optimum source amplitudes corresponding to the optimum radiation patterns of figure 8.

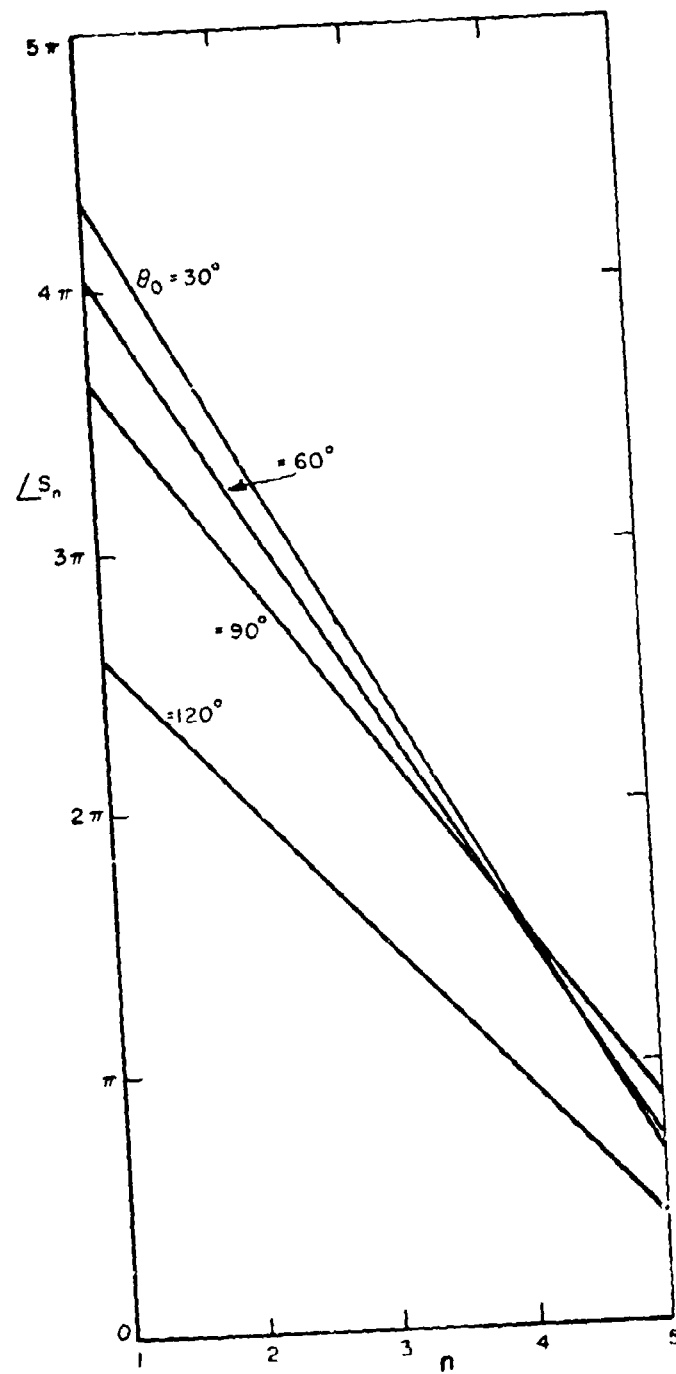


Figure 10. The optimum source phase distribution corresponding to the optimum radiation patterns of Figure 8.

of the impedance operator $Z = R + jX$ of the obstacle [10]. The function E_i is the i th characteristic field component tangential to the surface S . The characteristic currents (J_i) simultaneously yield orthonormal characteristic radiation patterns while they themselves have the orthonormality properties

$$(RJ_j, J_i)_{R_S} = \delta_{ij} \quad (61)$$

$$(XJ_j, J_i)_{R_S} = \lambda_i \delta_{ij} \quad (62)$$

where the inner product is still defined by Equation (2).

We next proceed to discuss the set of eigenfunctions of the Hermitian iterated operator as a set suitable for expanding fields radiated or scattered by a perfectly conducting obstacle. To begin, we note that the impedance operator Z relating current on S to tangential field on S is an example of the operator G described in Section II and so we can define eigensources and eigenfields in the manner already described. In this case, the eigensources are currents K_i on the obstacle surface and the associated eigenfields are components of the electric fields tangential to the same surface (making Z unbounded). The eigen-currents are solutions of Equation (6)

$$Z^* Z K_i = \nu_i K_i \quad (63)$$

satisfying the orthonormality conditions, (Equations (8) and (9))

$$(K_i, K_j)_{R_S} = \delta_{ij} \quad (64)$$

$$(K_i, Z^* Z K_j)_{R_S} = \nu_i \delta_{ij} \quad (65)$$

Note that the characteristic values λ_i are always real and can take values $-\infty \leq \lambda_i \leq \infty$, while the eigenvalues ν_i are always real and can take values $0 \leq \nu_i$. The characteristic values $\lambda_i = \pm \infty$ correspond to characteristic currents which resonate the interior volume of the obstacle while eigenvalues $\nu_i = 0$ correspond to this condition.

When the ambient medium is reciprocal, i.e., $z^* = z^C$, Equation (63) can be reduced to a simpler and instructive form. Operating on Equation (63) with z ,

$$\begin{aligned} z z^*(z K_i) &= \nu_i (z K_i) , \\ z z^C(z K_i) &= \nu_i (z K_i) \end{aligned} \quad (66)$$

and comparing this equation with Equation (63), conjugated,

$$z z^C K_i^C = \nu_i K_i^C \quad (67)$$

we see that $z K_i$ and K_i^C satisfy identical eigenvalue equations. This being so, they must be related by a multiplicative constant c_i , i.e.,

$$z K_i = c_i K_i^C \quad (68)$$

$$\hat{E}_i = c_i K_i^C$$

where \hat{E}_i is the i th eigenfield component tangential to the obstacle surface. The magnitudes of c_i are fixed by Equations (64) and (65) to be

$$|c_i|^2 = \nu_i \quad (69)$$

while the phases of c_i are not unique, being related to the arbitrary phases of K_i by Equation (68). Thus, we can choose the phases of c_i

for convenience. One possible choice is $c_i = jv_i^{1/2}$, purely imaginary quantities, in which case Equation (68) can be rewritten

$$\begin{bmatrix} X & R \\ R & -X \end{bmatrix} \begin{pmatrix} K_i' \\ K_i'' \end{pmatrix} = v_i^{1/2} \begin{pmatrix} K_i' \\ K_i'' \end{pmatrix} \quad (70)$$

where K_i' and K_i'' are the real and imaginary parts of K_i , respectively. Another possible choice is $c_i = v_i^{1/2} e^{j\gamma_i}$ where γ_i are chosen so that the phase of \tilde{E}_i is the negative of the phase of K_i , that is, the eigencurrent K_i and associated eigenfield \tilde{E}_i are scaled conjugate functions over S . This latter choice for c_i is general and provides an interesting contrast between eigenmodes of the Hermitian iterated operator and characteristic modes; namely, the real characteristic current J_i and its associated tangential field E_i maintain a constant phase difference over the surface S while their amplitude distributions differ in general over S ; on the other hand the generally complex eigencurrent K_i and its associated tangential field \tilde{E}_i maintain the same (scaled) amplitude distributions over S , while their phases vary over S in such a way as to make them conjugate functions.

For those special conducting shapes S , such as the sphere, the circular cylinder, the elliptic cylinder, etc, which correspond to constant coordinate surfaces of the separable coordinate systems, the characteristic currents J_i and eigencurrents K_i become identical (except for different real normalization constants) and their associated fields E_i and \tilde{E}_i become identical (except for different real normalization constants). Thus, the modal currents and fields on S track in both amplitude and phase. In such special cases, the ratio of the i th modal field and its current becomes a complex (in general) number which remains fixed over the entire surface and may be interpreted as the i th modal impedance $Z_i = R_i + jX_i$. Then Equations (58), (68) and (69), together with the choice $c_i = v_i^{1/2} e^{j\gamma_i}$ lead to

$$c_i = \sqrt{R_i^2 + X_i^2} e^{j \tan^{-1}(\frac{X_i}{R_i})} \quad (71)$$

or

$$v_i = (R_i^2 + X_i^2) \quad (72a)$$

and

$$\lambda_i = \frac{X_i}{R_i} \quad (72b)$$

which indicate the connection between the eigenvalues v_i of the Hermitian iterated operator and the characteristic values λ_i ,

$$c_i = R_i \sqrt{1 + \lambda_i^2} e^{j \tan^{-1} \lambda_i} \quad (73a)$$

or

$$v_i = R_i^2 (1 + \lambda_i^2) \quad (73b)$$

As examples, Equation (70) has been applied to a thin straight wire and infinite cylinder of rectangular cross section, using the method of moments [10] to arrive at matrix representations for \mathbf{g} and \mathbf{X} . Values of v_i are shown in Figures 11-13 as functions of electrical size of the obstacle. As expected in the case of the cylinder, where we pass through resonances of the interior region we notice that certain v_i become zero for kb corresponding to cut-off frequencies of associated waveguide modes. Those frequencies agree with theoretical values within 0.5% for the TM modes and within 0.24% for the TE modes, one quarter of the cylindrical periphery having been divided into 13 parts for application of the method of moments.

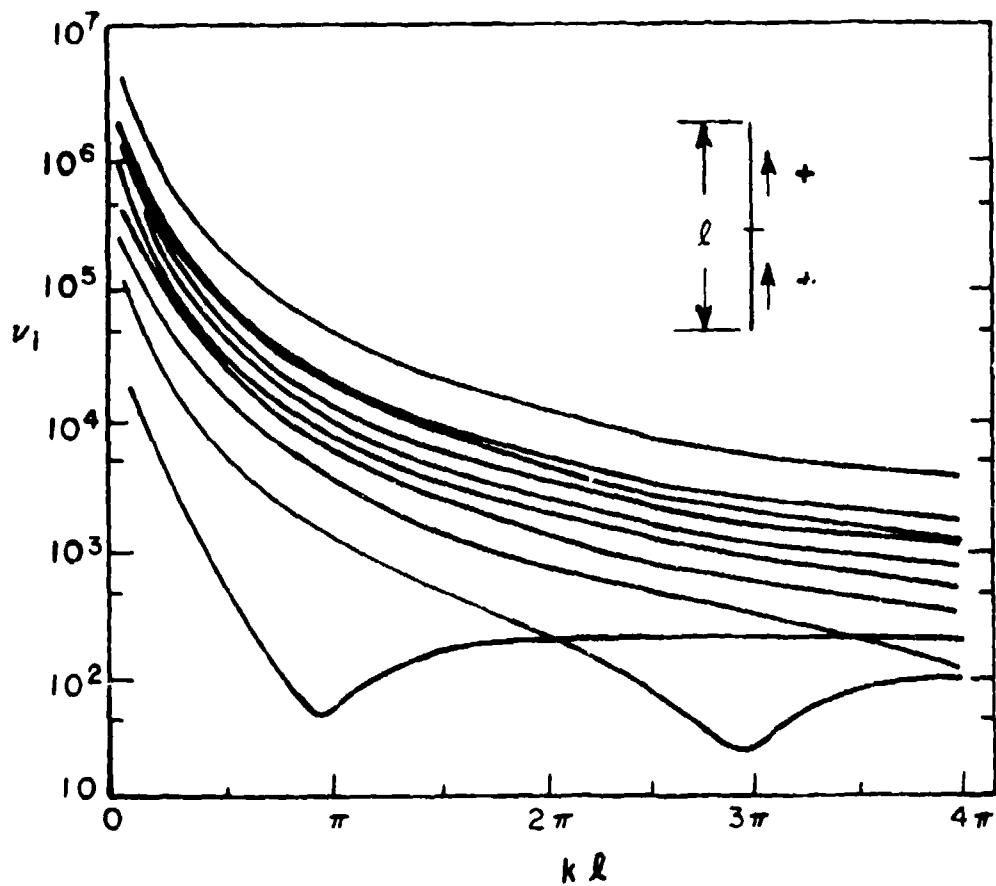


Figure 11. Eigenvalues for a straight wire with length l and $\Omega = 10$.
The number of subdivisions in the computation by the
moment method is 20 for the half-length.

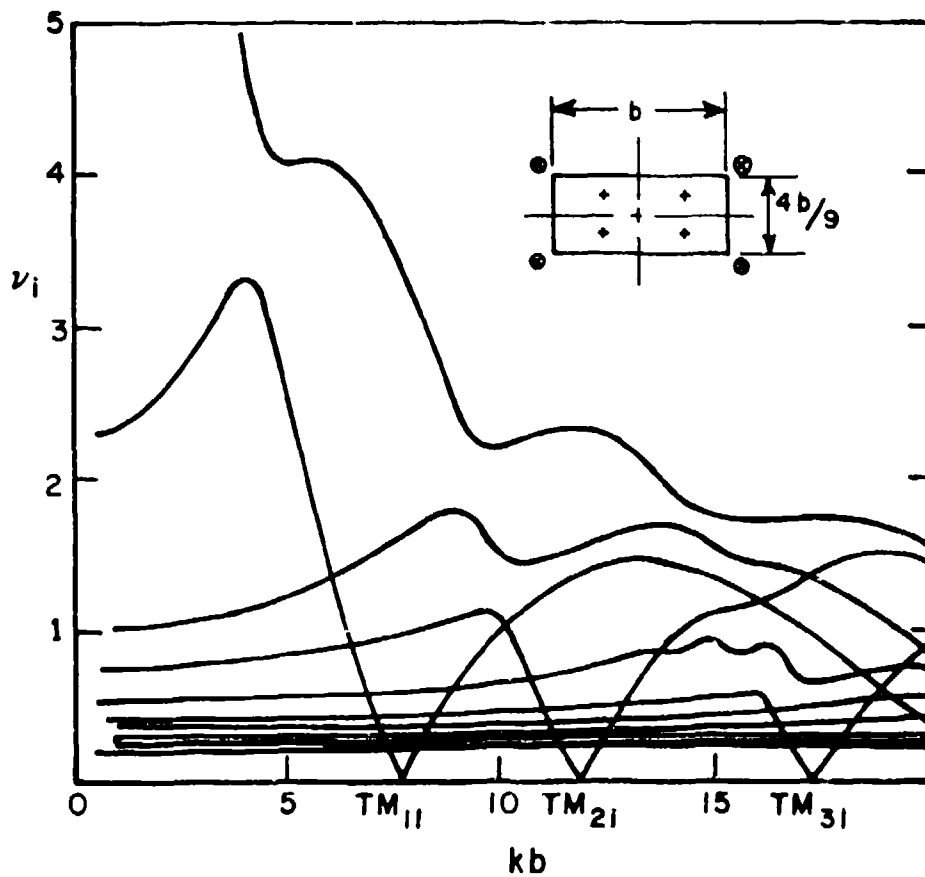


Figure 12. Eigenvalues of TM modes for a rectangular cylinder with side-lengths b and $4b/9$. The number of subdivisions in the computation by the moment method is 13 for one quarter of the periphery.

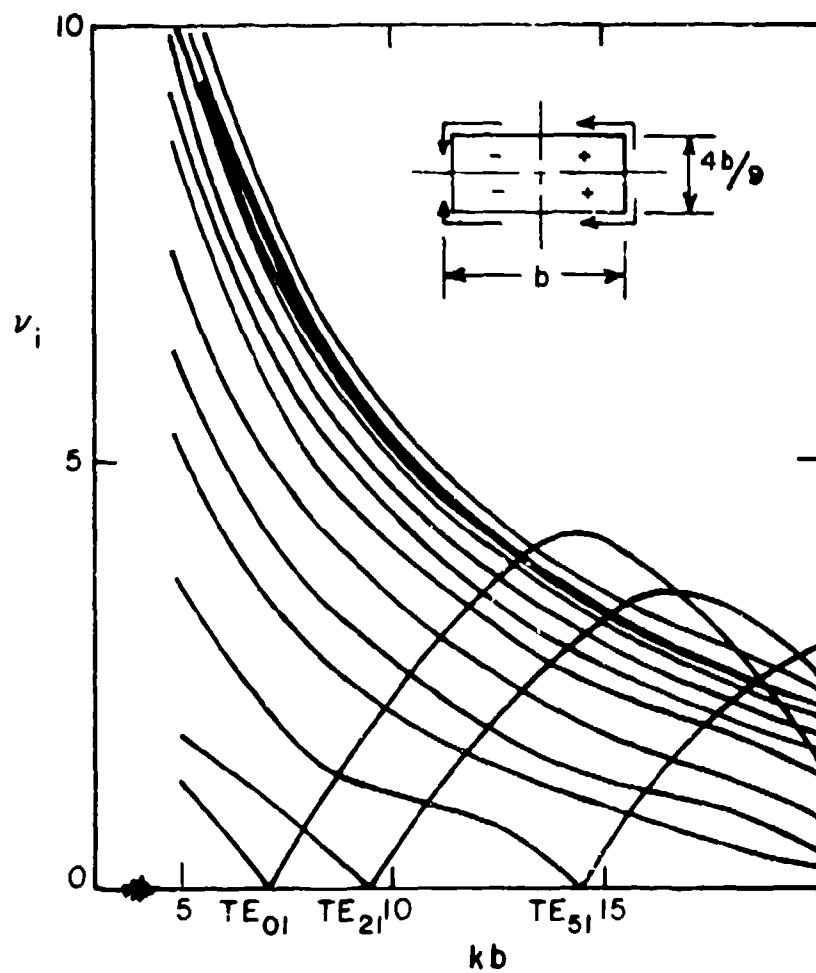


Figure 13. Eigenvalues of TE modes for a rectangular cylinder with side-lengths b and $4b/9$. The number of subdivisions in the computation by the moment method is 13 for one quarter of the periphery.

V. CONCLUSIONS

By extending Parseval's relation to any combination of a source and a field, we have arrived at an eigenvalue equation of a Hermitian operator formed by iterating any general operator relating a source and a field. The eigensources and corresponding eigenfields which are solutions to this eigenvalue equation are complete and orthogonal over the source and field regions, respectively. Any eigenvalue of the equation is the ratio of the norm of the corresponding eigenfield and the norm of the corresponding eigensource. Except when the operator is improperly singular, the completeness and orthogonality properties of the eigensolutions make them attractive for expanding arbitrary fields and sources associated with discrete or continuous radiating or scattering systems.

A few examples show the application of the theory to arrays and to two planar apertures. Out of the latter work comes the interesting observation that the theory applied to the operator equation known as the Fourier transform leads to eigenfunctions which are the prolate spheroidal functions.

When the theory is applied to the complex impedance matrix of a conducting scattering obstacle, it is shown that the eigencurrents and eigenfields introduced here are conjugates of each other, which contrast with characteristic currents and fields of Garbacz, Harrington and Mautz. Only in the case of obstacles corresponding to coordinates of separable coordinate systems do the two modal types coincide.

The eigenfunction theory is applied to the thin linear wire and the rectangular cylinder and the corresponding sets of eigenmodes are presented here. Results encourage the application of the theory to other shapes and invite an investigation of the eigencurrent distributions as well as the eigenvalues.

REFERENCES

1. R. J. Garbacz, "A Generalized Expansion for Radiated and Scattered Fields," Interaction Notes, No. 180, 1978; also Ph.D. dissertation, The Ohio State University, Columbus, Ohio 1968.
2. R. J. Garbacz and R. H. Turpin, "A Generalized Expansion for Radiated and Scattered Fields," IEEE Trans. Antennas and Propagation, Vol. AP-19, pp. 348-358, May 1971.
3. R. F. Harrington and J. R. Mautz, "Theory of Characteristic Modes for Conducting Bodies," IEEE Trans. Antennas and Propagation, Vol. AP-19, pp. 622-628, September 1971.
4. R. F. Harrington and J. R. Mautz, "Computation of Characteristic Modes for Conducting Bodies," IEEE Trans. Antennas and Propagation, Vol. AP-19, pp. 629-639, September 1971.
5. N. Inagaki, "Eigenfunction of Hermitian Iterated Operator and Its Application to Numerical Analysis," Digest of International Symposium on Antennas and Propagation, Japan, pp. 295-298, September 1978.
6. A. G. Fox and Tingye Li, "Resonant Modes in a Maser Interferometer," The Bell System Technical Journal, Vol. 40, pp. 453-488, March 1961.
7. D. Slepian and H. O. Pollak, "Prolate Spheroidal Wave Functions, Fourier Analysis and Uncertainty - I," The Bell System Technical Journal, Vol. 40, pp. 43-64, January 1961.

8. D. Slepian and Sonnenblack, "Eigenvalues Associated with Prolate Spheroidal Wave Functions of Zero Order," The Bell System Technical Journal, Vol. 44, pp. 1745-1759, October 1965.
9. D. K. Cheng and F. I. Tseng, "Gain Optimization for Arbitrary Antenna Arrays," IEEE Trans. Antennas and Propagation, Vol. AP-13, pp. 973-, November 1965.
10. R. F. Harrington, Field Computation by Moment Methods, the Macmillan Company, New York, 1968.